Author Manuscript

Author Manuscript

Author Manuscript

Author Manuscript

HHS Public Access

Author manuscript

Am J Med Genet A. Author manuscript; available in PMC 2020 February 21.

Published in final edited form as:

Am J Med Genet A. 2017 May ; 173(5): 1319–1327. doi:10.1002/ajmg.a.38207.

De Novo Loss-of-Function Variants in *STAG2* are Associated with Developmental Delay, Microcephaly and Congenital Anomalies

S. V. Mullegama[1,2,#], **S. Klein**[3,#], **M. V. Mulatinho**[1], **T.N. Senaratne**[1], **K. Singh**[4], **UCLA Clinical Genomics Center**[2], **D.C. Nguyen**[3], **N.M. Gallant**[4], **S.P. Strom**[1,2], **S. Ghahremani**[5], **P. N. Rao**[1], **J. A. Martinez-Agosto**[2,3,6,*]

[1]Department of Pathology and Laboratory Medicine, David Geffen School of Medicine, University of California, Los Angeles, Los Angeles, California, USA

[2]UCLA Clinical Genomics Center, David Geffen School of Medicine, University of California, Los Angeles, Los Angeles, California, USA

[3]Department of Human Genetics, David Geffen School of Medicine, University of California, Los Angeles, Los Angeles, California, USA

[4]Division of Genetic and Genomic Medicine, University of California, Irvine, California, USA, and Miller Children's and Women's Hospital Long Beach, Long Beach, California, USA

[5]Department of Radiology, David Geffen School of Medicine at UCLA, Los Angeles, California, USA

[6]Department of Pediatrics, David Geffen School of Medicine, University of California, Los Angeles, Los Angeles, California, USA

Abstract

The cohesin complex is an evolutionarily conserved multi-subunit protein complex which regulates sister chromatid cohesion during mitosis and meiosis. Additionally, the cohesin complex regulates DNA replication, DNA repair, and transcription. The core of the complex consists of four subunits; SMC1A, SMC3, RAD21, and STAG1/2. Loss-of-function mutations in many of these proteins have been implicated in human developmental disorders collectively termed "cohesinopathies". Through clinical exome sequencing of an 8-year-old girl with a clinical history of global developmental delay, microcephaly, microtia with hearing loss, language delay, ADHD, and dysmorphic features, we describe a heterozygous *de novo* variant (c.205C>T; p.(Arg69*)) in the integral cohesin structural protein, *STAG2*. This variant is associated with decreased STAG2 protein expression. Further, the analyses of metaphase spreads did not exhibit premature sister chromatid separation; however, delayed sister chromatid cohesion was observed. To further

[*]**Correspondence to:** Julian A. Martinez-Agosto MD, PhD, Address: 695 Charles E. Young Drive South, Gonda Research Center Room 4605, Los Angeles, CA 90095, Phone: 310-794-2405, Fax: 310-794-5446, julianmartinez@mednet.ucla.edu.
[#]Co-First Authors

Conflict of interest: No conflicts of interests

SUPPORTING INFORMATION

Additional supporting information may be found in the online version of this article at the publisher's web-site.

Author Manuscript Author Manuscript Author Manuscript Author Manuscript

support the pathogenicity of *STAG2* variants, we identified two additional female cases from the DECIPHER research database with mutations in *STAG2* and phenotypes similar to our patient. Interestingly, the clinical features of these three cases are remarkably similar to those observed in other well-established cohesinopathies. Herein, we suggest that *STAG2* is a dosage-sensitive gene and that heterozygous loss-of-function variants lead to a cohesinopathy.

Keywords

STAG2; cohesin complex; cohesin-associated genes; gene dosage; X-linked; cohesinopathy

INTRODUCTION

The cohesin complex is a large evolutionary conserved functional unit involved in DNA replication, gene expression, heterochromatin formation, DNA repair, and sister chromatid cohesion [Di Benedetto et al., 2013]. The cohesin complex consists of four core proteins, SMC1A, SMC3, RAD21 and STAG1/2 [Mannini et al., 2015a] (Figure 1A). In addition, there are several proteins that regulate the cohesin complex's interaction with chromosomes (*NIPBL, ESCO2, HDAC8, DDX11, SGOL1*, *WAPL*, *PDS5A, PLK1, AURKB* and *ATRX*) (Figure 1A) [Mannini et al., 2015b]. Loss-of-function mutations in these genes have been previously associated with multisystem developmental disorders termed "cohesinopathies" [Cucco and Musio 2016; Skibbens et al., 2013], including Cornelia de Lange syndrome (CdLS, MIM # 122470; *SMC1A, SMC3, NIPBL*, and *HDAC8*), Roberts/SC phocomelia syndrome (RBS MIM # 268300; *ESCO2*), α-thalassemia/mental retardation syndrome (ATRX, MIM # 301040; *ATRX*), Warsaw breakage syndrome (WBS, MIM # 613398; *DDX11*), Chronic Atrial and Intestinal Dysrhythmia (CAID, MIM # 616201; *SGOL1*), and Cornelia de Lange Syndrome 4 (CdLS4, MIM# 614701; *RAD21* mutations). [Ball et al., 2014; Barbero 2013; Gerkes et al., 2010; McNairn and Gerton 2008; Musio and Krantz 2010; Skibbens et al., 2013]. Overwhelmingly, these syndromes are characterized by decreased growth, limb malformations, developmental delay, dysmorphic features and behavioral phenotypes most specifically Attention Deficit Hyperactivity Disorder (ADHD).

One of the cohesin subunits in which loss-of-function mutations have yet to be associated with any cohesinopathies is the stromal antigen 2 gene (MIM # 300826; *STAG2*). Recently, 33 chromosome Xq25 duplications involving *STAG2* and *STAG2*-only duplications have been identified in males with intellectual disability, behavioral problems, seizures, malar flatness and prognathism [Bonnet et al., 2009; Kumar et al., 2015; Leroy et al., 2016; Philippe et al., 2013; Yingjun et al., 2015]. The genetic and molecular data in these studies provide compelling evidence that *STAG2* may be a dosage sensitive gene [Kumar et al., 2015]. However, no *STAG2* loss-of-function or missense mutations have been identified in individuals with multisystem anomalies and neurodevelopmental delays.

Here, we describe *de novo* loss-of-function heterozygous *STAG2* variants associated with developmental delay, deafness, craniofacial abnormalities, and congenital heart defects.

Author Manuscript Author Manuscript Author Manuscript Author Manuscript

METHODS

Patient Ascertainment

All samples and information were collected after informed consent was obtained and in accordance with local Institutional Review Board (IRB) approved protocols from the University of California, Los Angeles. The clinical assessment included a review of medical records, including developmental, biochemical, neurological, and genetic evaluations. Fresh peripheral blood samples for molecular and cytogenetic studies were collected from the proband and her mother and father.

Clinical Exome Sequencing (CES)

CES was performed at the UCLA Clinical Genomics Center, on DNA of the affected girl and both parents, as previously described [Lee et al., 2014]. Briefly, exome capture was performed using Agilent SureSelect XT Clinical Research Exome, sequencing was performed on HiSeq2500 as 100bp paired end runs and variant annotation was performed using GoldenHelix SNP & Variation Suite [Lee et al., 2014; Rehm et al., 2013]. Rareness of the variant in the population was measured using the minor allele frequency (MAF) score from Exome Aggregation Consortium (ExAC) database. Variants with greater than 1% MAF in this database were considered common and removed from the final candidate list. In total 23,398 DNA variants were identified, including 21,727 single nucleotide substitutions and 1,671 small deletions/insertions (1–10bp). The data are consistent with a high quality genomic sequence and fall within normal human genomic variation quality parameters.

Sanger Sequencing

Genomic DNA from the proband and her parents was extracted from peripheral blood using standard protocols. Exon 5 and adjacent intron boundaries of *STAG2* (RefSeq NM_001042749.1) were sequenced using Big Dye Terminator V1.1 cycle sequencing kit and ABI3130×l genetic analyzer following manufacturers guidelines. Primers and PCR conditions are available upon request. The sequencing results were processed with the 4Peaks software (http://nucleobytes.com/4peaks/).

Western Blot Analysis

Venous blood was drawn from the proband and both parents, and immediately spun at 100g for 20 minutes for from platelet rich plasma (PRP). One milliliter of the PRP was transferred to a 1.5ml Eppendorf tube and spun at 100g for 20 minutes to pellet the white blood cells. The supernatant was discarded and the pellet was suspended in 500μl of passive lysis buffer, prepared with phosphatase and protease inhibitors, and incubated by shaking at 4°C for one hour. After lysis tubes were spun at 7500 Rcf for 5 minutes to collect debris. Supernatant was transferred to a new tube then protein concentration determined with the Coommasie Plus Bradford (Life Technologies) reagent following manufacture instructions. Western blots were run on 12% acrylamide gels followed by transfer onto nitrocellulose membranes utilizing the Transblot Turbo® apparatus from Biorad. The membrane was blocked in 5% bovine serum albumin in Tris buffered saline plus Tween (TBST) for 30 minutes, then incubated with either of two independent primary antibodies against STAG2 (Cell Signaling

Author Manuscript Author Manuscript Author Manuscript Author Manuscript

#4239 Dilution 1/500 and Cell Signaling #5882 Dilution 1/500) and beta-actin (Cell Signaling #4970, Dilution 1/5000) for 24 hours. Blots were then rinsed with Tris buffered saline (TBS) and washed three times with TBST. Blots were then incubated in rabbit secondary antibodies conjugated to horseradish peroxidase at a dilution of 1/3750. Following secondary incubation membranes were rinsed with TBS then washed twice with TBST. Blots were exposed using Western Clarity reagents from BioRad and imaged on the Bio Rad ChemiDoc and viewed in ImageLab Software. Quantification of band intensity was performed using ImageLab with each band normalized to its independent loading control. Statistical analysis was performed on averages derived from six technical replicates using the Mann-Whitney U Test.

Immunofluorescence

One hundred thousand human neural stem cells were plated on GelTrex (Invitrogen) coated coverslips. After 24 hours of growth cells were fixed using paraformaldehyde for 20 minutes then blocked with 10% normal goat serum in TBST overnight. The following day coverslips were washed three times in TBST. Coverslips were incubated in primary antibody against STAG2 (Cell Signaling #5882 Dilution 1/250) in 3% BSA in TBST for one hour. Coverslips were then washed three times in TBST and incubated in secondary antibody (Jackson Laboratories, AffiniPure Donkey Anti-Rabbit, 711-165-152, Dilution 1/1000 and Invitrogen, Alexa Fluor® 647 Phalloidin, A22287, dilution 1/100) in 3% BSA in TBST for one hour. Coverslips were then washed three times in TBST and then three times in water. Coverslips were mounted on glass slides using ProLong® Gold Antifade Mountant with DAPI (Invitrogen, P36931). Slides were imaged using a Zeiss LSM-800.

Cytogenetic Studies

Wright-Giemsa stained metaphase cells were prepared from PHA-stimulated cultures of peripheral blood from the proband and parents following routine G-banding protocols to determine the karyotype status of the three individuals. For sister chromatid cohesion assays, for each of the three individuals, 60 metaphase cells in which each chromosome could be clearly resolved as two chromatids were scored. Individual chromosomes were examined for cohesion between the sister chromatids (SC), paying close attention to the centromeric regions. A chromosome was scored as showing complete separation (“open”) if the two chromatids were clearly unattached along their entire length including the centromeric region. A chromosome was scored as showing “partial” separation if one or both SCs showed lack of a centromeric constriction and a potential gap between the SCs was visible at the centromere. For each metaphase cell, the numbers of open, partial, and closed chromosome pairs were scored. Cells were analyzed independently by two observers (once in a blinded fashion). The cells were classified as having premature sister chromatid separation (PSCS) if at least three chromosome pairs per metaphase cell showed the open or partial phenotype, while cells were classified as intermediate if one or two chromosome pairs showed the open or partial phenotype. Statistical analyses were conducted using two-tailed Fisher’s Exact tests.

Author Manuscript Author Manuscript Author Manuscript Author Manuscript

RESULTS

Patient report

Case 1 was a female born at 40 weeks gestation to a via caesarean section to a 21-year-old primagravida mother and a 23 year-old father. Pregnancy was not significant for any major medical problems, tetratogenic exposures or hospitalizations. The parents were Latino/Hispanic and family history was negative for any significant morbidities or consanguinity (Figure 1B). Birth weight was 3,629 g (50^{th}–75^{th} centile) and length 51 cm (50^{th}–75^{th} centile). She was admitted to the neonatal intensive care unit (NICU) because of apnea and feeding problems. Examination by a medical geneticist in the NICU documented bilateral microtia (grade 1 on the right and grade 3 on the left), left preauricular pit and tag, left facial palsy (with left eye unable to close), bilateral paramedian lower lip pits, and submucous cleft palate with bifid uvula. Testing revealed abnormal newborn hearing screen. Brain MRI on day two of life showed dysgenesis of the splenium of the corpus callosum (Figure 2 A–B). Posterior to the splenium was an 18mm interventricular subarachnoid cyst and a subgaleal hematoma at the cortex. Echocardiogram showed an apical and muscular ventricular septal defect and chest x-ray showed multiple thoracic vertebral anomalies (Figure 2 C–D). Abdominal ultrasound in the neonatal period showed mild left pelviectasis. She was discharged after two weeks in the NICU and development was followed: she smiled at 2 months, rolled over at 6 months, sat without support at age 8 months, crawled at 1 year, stood and walked independently at 18 months, and spoke her first words at 18 months. At age 2 years 7 months a developmental evaluation showed delays in expressive language but no deficits in other areas and no signs of autism were appreciated. At age 4, evaluation of the microtia included a CT scan of the temporal bones that showed left external auditory canal atresia with a fused ossicular mass, absent stapes, and severely stenotic oval window. There was a small pneumatized and aerated middle ear cavity and mastoid antrum. The tympanic segment of the facial nerve was asymmetrically small without normal communication with the anterior genu. On the right, there was absence of the stapes and severe stenosis or absence of the oval window with a medially placed tympanic segment of the facial nerve (Figure 2 E–G). At 6 years old, her abdominal ultrasound was repeated and showed left pelviectasis resolution. At 8-years-old, her weight was 24.5 kg (29^{th} centile), and length was 121.7 cm (8^{th} centile) and her head circumference was 48 cm (5^{th} centile) demonstrating decelerating brain growth and borderline microcephaly and undergrowth. Physical exam at that time was notable for a low anterior hairline, sloping forehead, left eye smaller than the right, asymmetric facial movements, and bilateral fifth finger clinodactyly. She had radiological evidence of scoliosis (Figure 2 H–I). Her receptive language was intact but she continued to require speech therapy at school due to delays in expressive language. She was diagnosed with Attention Deficit Hyperactivity Disorder. Karyotype showed a normal female (46,XX). Chromosomal microarray on both BAC and SNP platforms were normal.

Clinical Exome Sequencing identifies a *de novo* loss-of-function heterozygous variant in *STAG2*

CES performed on Case 1 revealed a *de novo* heterozygous variant in the *STAG2* gene (NM_001042749.1: c.205C>T, p.Arg69*; Supplementary Table I). Sanger sequencing analysis of this variant in the parental samples did not detect the variant, suggesting that the

Author Manuscript Author Manuscript Author Manuscript Author Manuscript

change arose *de novo* in this patient (Figure 1B). Exome Aggregation Consortium (ExAC) has given this gene a predicted LoF pLI score of 1.00 to suggest loss of function variants in healthy individuals are rare. The c.205C>T, p.Arg69* variant results in a stop-gain (nonsense) change which results in a truncated, predicted non-functional protein product (Figure 3A). The three essential domains of STAG2 (stromal antigen 2 domain, stromalin conservative domain, and glutamine rich domain) are not present due to this mutation (Figure 1A). Upon searching the DECIPHER database (https://decipher.sanger.ac.uk), we identified two *de novo* heterozygous *STAG2* variants in two female cases that had phenotype information described in Human Phenotype Ontology (HPO) terms (Table I). Case 2 has a missense variant; c.1811G>A, p.Arg604Gln (Figure 3A and Supplementary Table I) [Deciphering Developmental Disorders 2015]. SIFT and PolyPhen-2 predicted the c.1811G>A (p.Arg604Gln) missense variant to be deleterious and probably damaging (Supplementary Table I). Case 3 has a frameshift variant that results in a truncated protein product; c.1913_1922del, (p.Ala638Valfs*10) (Figure 3A and Supplementary Table I). The glutamine rich (GR) domain in STAG2, known to be an activation domain of transcription factors [Xiao and Jeang 1998], is not present due to Case 3's mutation, which consequently could affect the transcriptional functions of STAG2 (Figure 3A). All three variants are absent from public databases including Exome Aggregation Consortium (ExAC) and 1000 Genome Project [Abecasis et al., 2012]. Since *STAG2* variants had yet to be associated with any clinical condition, these variants were classified as variants of unknown clinical significance (VOUS) based on the American College of Medical Genetics and Genomics variant assessment [Richards et al., 2015] (Supplementary Table I).

Haploinsufficiency of *STAG2* is likely pathogenic

The ExAC database demonstrates that *STAG2* is extremely intolerant to loss of function variants in healthy populations (43 individuals expected, zero observed), suggesting that haploinsufficiency is likely pathogenic. Further, the DECIPHER database has given *STAG2* a haploinsufficiency score (HI index) of 9.66%, which is a high rank (e.g. 0–10%), indicating the gene is more likely to exhibit haploinsufficiency [Huang et al., 2010].

It is expected that Case 1's *STAG2* variant results in a premature termination of translation (Figure 3A). It is likely that nonsense mediated decay could be occurring due this mutation or we could either see the synthesis of a truncated protein lacking the last 1172 amino acids (Figure 3A). Western blot analysis confirmed that the mutation is most likely pathogenic as the protein samples prepared from the proband contain less STAG2 than either parent control (Figure 3B–C). Lastly, no alternative splice or truncated variants of smaller size were observed via western blot analysis (Data not shown) indicating that the c.205C>T variant reduces STAG2 protein expression *in vivo*. However, we cannot rule out the possibility that nonsense mediated decay is occurring.

Effect of *STAG2* haploinsufficiency on sister chromatid cohesion

Since it is well established that *STAG2* encodes a subunit of cohesin, a complex that mediates sister chromatid cohesion to ensure accurate chromosome segregation, we next determined if the p.Arg69* variant affects SC cohesion by analyzing metaphase cells for indications of premature sister chromatid separation (PSCS). For each metaphase cell, all

Author Manuscript Author Manuscript Author Manuscript Author Manuscript

sister chromatid pairs were examined to determine if there was no separation ("closed"), clear premature separation at the centromere ("open"), or an intermediate ("partial") phenotype, respectively. Cells were then classified into three categories based on the numbers of chromosome pairs showing the different phenotypes (Figure 4; see Methods for more details). These studies found that the proband did not show increased PSCS when compared to the parents (Figure 4D). However, the number of metaphases in the PSCS category was significantly reduced in the proband compared to controls (patient versus mother, p= 0.000029; patient versus father, p= 0.00075) (Figure 4D). It was then hypothesized that the *STAG2* mutation may have resulted in tighter sister chromatid cohesion. Importantly, the karyotypes were all cytogenetically normal, and there were no significant aneuploidies observed in metaphases from the proband or from the parents.

DISCUSSION

Here, we describe *de novo* heterozygous likely pathogenic *STAG2* variants associated with a phenotype that is associated with nervous system (HP:0000707), head or neck (HP:0000152) and ear (HP:0000598) abnormalities (Table I). More specifically, the phenotypes include microcephaly, microtia with hearing loss, developmental delay, language delay, ADHD, and dysmorphic features, overlapping with established cohesinopathies (Table II).

Characterization of our *STAG2* variant indicates a loss-of-function mechanism due to decreased STAG2 protein expression. Furthermore, our cytogenetic studies did not reveal significant amounts of PSCS but did show that the mutant cells had tighter sister chromatid cohesion. The contribution of this alteration in chromosome segregation to the phenotype is not yet fully understood and is complicated by the multi-functional nature of STAG2. For example, *STAG2* is also a transcription factor and mutations could affect its binding to specific DNA sequences crucial for proper neurodevelopment and craniofacial development. Additionally, STAG2 is the only cohesin subunit that interacts directly with the zinc finger DNA binding protein (CTCF) [Lake et al., 2016; Ong and Corces 2014; Van Bortle et al., 2015]. CTCF is required for cohesion dependent insulation activity and CTCF mutations have been indirectly implicated in intellectual disability [Van Bortle et al., 2015]. About 50–80% of CTCF binding sites in the genome are occupied by the cohesin complex [Lake et al., 2016; Ong and Corces 2014; Van Bortle et al., 2015]. Thus, a nonfunctional cohesin complex results in the disruption of CTCF-mediate intrachromosomal interactions [Lake et al., 2016; Ong and Corces 2014; Van Bortle et al., 2015]. We propose that disruption of STAG2's other functions, such as the regulation of gene expression, may contribute more to the phenotype than the effects on sister chromatin segregation similarly noted in other cohesinopathy genes [Deardorff et al., 2012; Remeseiro et al., 2013; Skibbens et al., 2013].

Additionally, from this work, we have shown that not all mutations in cohesin complex core subunits affect sister chromatid separation equally. The cellular phenotype most recently described with *RAD21* mutations was not replicated in our analysis [Deardorff et al., 2012]. This further suggests that the cohesin complex as a whole may affect global transcription and its alterations converge on transcriptional deregulation of key developmental genes. The lack of consensus on sister chromatid separation cellular phenotypes despite overwhelming clinical overlap leads us to believe that there is an additional mechanism contributing to

Author Manuscript Author Manuscript Author Manuscript Author Manuscript

cohesinopathy-associated phenotypes. Furthermore, comparison of *STAG2* associated phenotypes with those of well-known cohesinopathies, revealed an overall phenotypic gestalt which is remarkably similar, suggesting common molecular etiologies (Table II).

Recently 33 chromosome Xq25 duplications involving *STAG2* have been identified in males with intellectual disability, behavioral problems, seizures, malar flatness and prognathism [Bonnet et al., 2009; Kumar et al., 2015; Leroy et al., 2016; Philippe et al., 2013; Yingjun et al., 2015]. In this study, we illustrate how *STAG2* LOF variants can lead to a phenotype as well. Comparing the phenotype of loss-of-function variants in *STAG2* to *STAG2* duplications, we see that while there is a slight overlap of phenotypic features in these *STAG2* patients, the phenotype of loss-of-function variants in *STAG2* result in a more severe phenotype than *STAG2* duplications and is more similar to other cohesinopathies (Table I and Supplementary Table II). Based on this study, we suggest that *STAG2* should be added to the expanding list of dosage-sensitive genes that are responsible for neurodevelopmental disorders [Vissers and Stankiewicz 2012].

Finally, the number of X-linked genes in which *de novo* mutations cause disorders specifically in females are limited [Grozeva et al., 2015; Kumar et al., 2015; Tzschach et al., 2015]. The utilization of next generation sequencing methods has increased the identification of novel X-linked gene mutations in females with developmental delay with multiple congenital malformations [Retterer et al., 2016; Yang et al., 2013]. *STAG2* is a gene located on chromosome Xq25. From studies that have determined X-chromosome inactivation (XCi) status of over 400 X-linked genes, *STAG2* was found to be a gene that undergoes inactivation [Cotton et al., 2013]. In our study, all our cases are females with *de novo* heterozygous mutations in *STAG2*. It is conceivable that pathogenic loss-of-function *STAG2* variants that affect canonical STAG, SCD and GR domains are lethal in males with a 46,XY karyotype similar to males with pathogenic loss-of-function *MECP2* variants in canonical MBD and TRD domains are considered to be lethal [Bianciardi et al., 2016] (Rett syndrome; MIM 300005). Furthermore, the variable clinical severity in both females and males could be dependent on the type of variant (missense versus truncation), location (within a functional domain) and skewed XCi [Chae et al., 2004; Weaving et al., 2003]. For example, a female that carries a pathogenic *STAG2* variant but has favorably skewed XCi may have mild or no symptoms. Interestingly, *STAG2* was thought to undergo skewed XCi, however, a clinical test of our patient. Additionally, *STAG2* male cases that are mosaic or have a 47,XXY karyotype could possibly exist and have a milder phenotype.

Overall, our findings solidify that *STAG2* is a dosage sensitive gene and furthermore provide evidence that loss-of-function mutations in *STAG2* result in a cohesinopathy. The shared phenotype includes abnormalities of the nervous system, head, neck and ear. Additional features identified in the DECIPHER cases was limited to standardized terms from the Human Phenotype Ontology. This information has the benefit of standardizing phenotypes and allowing for coded data sharing. However, it also introduces generalizations that lack specific clinical details. Despite this, the shared phenotypic data as presented in Table I suggests that these variants are likely pathogenic and furthermore contribute to the disease process. Further studies on the cellular and molecular function of STAG2, and other cohesin

Author Manuscript Author Manuscript Author Manuscript Author Manuscript

complex components, may reveal the exact mechanism of dosage sensitivity and its effects on normal development.

Supplementary Material

Refer to Web version on PubMed Central for supplementary material.

ACKNOWLEDGEMENTS

We are very grateful to the family who contributed to this study. This work was supported by March of Dimes (grant #6-FY12-324, JAM-A), UCLA Children's Discovery Institute, UCLA CART (NIH/NICHD grant# P50-HD-055784, JAM-A), NIH/NCATS UCLA CTSI (Grant # UL1TR000124, JAM-A), Autism Speaks grant #9172 (SK) and the UCLA-Caltech MSTP NIH T32GM008042 (SK). The confocal images were acquired using the UCLA IDDRC/UCTraN Microscopy Core, supported by the NICHD/NIH U54 grant, HD087101, LSM-800.

REFERENCES

Ball AR Jr., Chen YY, Yokomori K. 2014 Mechanisms of cohesin-mediated gene regulation and lessons learned from cohesinopathies. Biochim Biophys Acta 1839(3):191–202. [PubMed: 24269489]

Barbero JL. 2013 Genetic basis of cohesinopathies. Appl Clin Genet 6:15–23. [PubMed: 23882154]

Bonnet C, Leheup B, Beri M, Philippe C, Gregoire MJ, Jonveaux P. 2009 Aberrant GRIA3 transcripts with multi-exon duplications in a family with X-linked mental retardation. Am J Med Genet A 149A(6):1280–1289. [PubMed: 19449417]

Chae JH, Hwang H, Hwang YS, Cheong HJ, Kim KJ. 2004 Influence of MECP2 gene mutation and X-chromosome inactivation on the Rett syndrome phenotype. J Child Neurol 19(7):503–508. [PubMed: 15526954]

Cotton AM, Ge B, Light N, Adoue V, Pastinen T, Brown CJ. 2013 Analysis of expressed SNPs identifies variable extents of expression from the human inactive X chromosome. Genome Biol 14(11):R122. [PubMed: 24176135]

Cucco F, Musio A. 2016 Genome stability: What we have learned from cohesinopathies. Am J Med Genet C Semin Med Genet 172(2):171–178. [PubMed: 27091086]

Deardorff MA, Wilde JJ, Albrecht M, Dickinson E, Tennstedt S, Braunholz D, Monnich M, Yan Y, Xu W, Gil-Rodriguez MC, Clark D, Hakonarson H, Halbach S, Michelis LD, Rampuria A, Rossier E, Spranger S, Van Maldergem L, Lynch SA, Gillessen-Kaesbach G, Ludecke HJ, Ramsay RG, McKay MJ, Krantz ID, Xu H, Horsfield JA, Kaiser FJ. 2012 RAD21 mutations cause a human cohesinopathy. Am J Hum Genet 90(6):1014–1027. [PubMed: 22633399]

Deciphering Developmental Disorders S. 2015 Large-scale discovery of novel genetic causes of developmental disorders. Nature 519(7542):223–228. [PubMed: 25533962]

Di Benedetto D, Di Vita G, Romano C, Giudice ML, Vitello GA, Zingale M, Grillo L, Castiglia L, Musumeci SA, Fichera M. 2013 6p22.3 deletion: report of a patient with autism, severe intellectual disability and electroencephalographic anomalies. Mol Cytogenet 6(1):4. [PubMed: 23324214]

Gerkes EH, van der Kevie-Kersemaekers AM, Yakin M, Smeets DF, van Ravenswaaij-Arts CM. 2010 The importance of chromosome studies in Roberts syndrome/SC phocomelia and other cohesinopathies. Eur J Med Genet 53(1):40–44. [PubMed: 19878742]

Grozeva D, Carss K, Spasic-Boskovic O, Tejada MI, Gecz J, Shaw M, Corbett M, Haan E, Thompson E, Friend K, Hussain Z, Hackett A, Field M, Renieri A, Stevenson R, Schwartz C, Floyd JA, Bentham J, Cosgrove C, Keavney B, Bhattacharya S, Italian XlMRP, Consortium UK, Consortium G, Hurles M, Raymond FL. 2015 Targeted Next-Generation Sequencing Analysis of 1,000 Individuals with Intellectual Disability. Hum Mutat 36(12):1197–1204. [PubMed: 26350204]

Kumar R, Corbett MA, Van Bon BW, Gardner A, Woenig JA, Jolly LA, Douglas E, Friend K, Tan C, Van Esch H, Holvoet M, Raynaud M, Field M, Leffler M, Budny B, Wisniewska M, Badura-Stronka M, Latos-Bielenska A, Batanian J, Rosenfeld JA, Basel-Vanagaite L, Jensen C, Bienek M, Froyen G, Ullmann R, Hu H, Love MI, Haas SA, Stankiewicz P, Cheung SW, Baxendale A,

Author Manuscript Author Manuscript Author Manuscript Author Manuscript

Nicholl J, Thompson EM, Haan E, Kalscheuer VM, Gecz J. 2015 Increased STAG2 dosage defines a novel cohesinopathy with intellectual disability and behavioral problems. Hum Mol Genet 24(25):7171–7181. [PubMed: 26443594]

Lake RJ, Boetefuer EL, Won KJ, Fan HY. 2016 The CSB chromatin remodeler and CTCF architectural protein cooperate in response to oxidative stress. Nucleic Acids Res 44(5):2125–2135. [PubMed: 26578602]

Lee H, Deignan JL, Dorrani N, Strom SP, Kantarci S, Quintero-Rivera F, Das K, Toy T, Harry B, Yourshaw M, Fox M, Fogel BL, Martinez-Agosto JA, Wong DA, Chang VY, Shieh PB, Palmer CG, Dipple KM, Grody WW, Vilain E, Nelson SF. 2014 Clinical exome sequencing for genetic identification of rare Mendelian disorders. JAMA 312(18):1880–1887. [PubMed: 25326637]

Leroy C, Jacquemont ML, Doray B, Lamblin D, Cormier-Daire V, Philippe A, Nusbaum S, Patrat C, Steffann J, Colleaux L, Vekemans M, Romana S, Turleau C, Malan V. 2016 Xq25 duplication: the crucial role of the STAG2 gene in this novel human cohesinopathy. Clin Genet 89(1):68–73. [PubMed: 25677961]

Mannini L, Cucco F, Quarantotti V, Amato C, Tinti M, Tana L, Frattini A, Delia D, Krantz ID, Jessberger R, Musio A. 2015a SMC1B is present in mammalian somatic cells and interacts with mitotic cohesin proteins. Sci Rep 5:18472. [PubMed: 26673124]

Mannini, L CL F, Cucco F, Amato C, Quarantotti V, Rizzo IM, Krantz ID, Bilodeau S, Musio A. 2015b Mutant cohesin affects RNA polymerase II regulation in Cornelia de Lange syndrome. Sci Rep 5:16803. [PubMed: 26581180]

McNairn AJ, Gerton JL. 2008 Cohesinopathies: One ring, many obligations. Mutat Res 647(1–2):103–111. [PubMed: 18786550]

Musio A, Krantz ID. 2010 Cohesin biology and the cohesinopathies: Abstracts from the Second Biennial Conference, Pontignano, Italy, 2009. Am J Med Genet A 152A(7):1630–1640. [PubMed: 20583191]

Ong CT, Corces VG. 2014 CTCF: an architectural protein bridging genome topology and function. Nat Rev Genet 15(4):234–246. [PubMed: 24614316]

Philippe A, Malan V, Jacquemont ML, Boddaert N, Bonnefont JP, Odent S, Munnich A, Colleaux L, Cormier-Daire V. 2013 Xq25 duplications encompassing GRIA3 and STAG2 genes in two families convey recognizable X-linked intellectual disability with distinctive facial appearance. Am J Med Genet A 161A(6):1370–1375. [PubMed: 23637084]

Rehm HL, Bale SJ, Bayrak-Toydemir P, Berg JS, Brown KK, Deignan JL, Friez MJ, Funke BH, Hegde MR, Lyon E, Working Group of the American College of Medical G, Genomics Laboratory Quality Assurance C. 2013 ACMG clinical laboratory standards for next-generation sequencing. Genet Med 15(9):733–747. [PubMed: 23887774]

Remeseiro S, Cuadrado A, Losada A. 2013 Cohesin in development and disease. Development 140(18):3715–3718. [PubMed: 23981654]

Renault NK, Renault MP, Copeland E, Howell RE, Greer WL. 2011 Familial skewed X-chromosome inactivation linked to a component of the cohesin complex, SA2. J Hum Genet 56(5):390–397. [PubMed: 21412246]

Retterer K, Juusola J, Cho MT, Vitazka P, Millan F, Gibellini F, Vertino-Bell A, Smaoui N, Neidich J, Monaghan KG, McKnight D, Bai R, Suchy S, Friedman B, Tahiliani J, Pineda-Alvarez D, Richard G, Brandt T, Haverfield E, Chung WK, Bale S. 2016 Clinical application of whole-exome sequencing across clinical indications. Genet Med 18(7):696–704. [PubMed: 26633542]

Richards S, Aziz N, Bale S, Bick D, Das S, Gastier-Foster J, Grody WW, Hegde M, Lyon E, Spector E, Voelkerding K, Rehm HL, Committee ALQA. 2015 Standards and guidelines for the interpretation of sequence variants: a joint consensus recommendation of the American College of Medical Genetics and Genomics and the Association for Molecular Pathology. Genet Med 17(5):405–424. [PubMed: 25741868]

Skibbens RV, Colquhoun JM, Green MJ, Molnar CA, Sin DN, Sullivan BJ, Tanzosh EE. 2013 Cohesinopathies of a feather flock together. PLoS Genet 9(12):e1004036. [PubMed: 24367282]

Tzschach A, Grasshoff U, Beck-Woedl S, Dufke C, Bauer C, Kehrer M, Evers C, Moog U, Oehl-Jaschkowitz B, Di Donato N, Maiwald R, Jung C, Kuechler A, Schulz S, Meinecke P, Spranger S, Kohlhase J, Seidel J, Reif S, Rieger M, Riess A, Sturm M, Bickmann J, Schroeder C, Dufke A,

Author Manuscript Author Manuscript Author Manuscript Author Manuscript

Riess O, Bauer P. 2015 Next-generation sequencing in X-linked intellectual disability. Eur J Hum Genet 23(11):1513–1518. [PubMed: 25649377]

Van Bortle K, Peterson AJ, Takenaka N, O'Connor MB, Corces VG. 2015 CTCF-dependent co-localization of canonical Smad signaling factors at architectural protein binding sites in D. melanogaster. Cell Cycle 14(16):2677–2687. [PubMed: 26125535]

Vissers LE, Stankiewicz P. 2012 Microdeletion and microduplication syndromes. Methods Mol Biol 838:29–75. [PubMed: 22228006]

Weaving LS, Williamson SL, Bennetts B, Davis M, Ellaway CJ, Leonard H, Thong MK, Delatycki M, Thompson EM, Laing N, Christodoulou J. 2003 Effects of MECP2 mutation type, location and X-inactivation in modulating Rett syndrome phenotype. Am J Med Genet A 118A(2):103–114. [PubMed: 12655490]

Xiao H, Jeang KT. 1998 Glutamine-rich domains activate transcription in yeast Saccharomyces cerevisiae. J Biol Chem 273(36):22873–22876. [PubMed: 9722505]

Yang Y, Muzny DM, Reid JG, Bainbridge MN, Willis A, Ward PA, Braxton A, Beuten J, Xia F, Niu Z, Hardison M, Person R, Bekheirnia MR, Leduc MS, Kirby A, Pham P, Scull J, Wang M, Ding Y, Plon SE, Lupski JR, Beaudet AL, Gibbs RA, Eng CM. 2013 Clinical whole-exome sequencing for the diagnosis of mendelian disorders. N Engl J Med 369(16):1502–1511. [PubMed: 24088041]

Yingjun X, Wen T, Yujian L, Lingling X, Huimin H, Qun F, Junhong C. 2015 Microduplication of chromosome Xq25 encompassing STAG2 gene in a boy with intellectual disability. Eur J Med Genet 58(2):116–121. [PubMed: 25450604]

Author Manuscript Author Manuscript Author Manuscript Author Manuscript

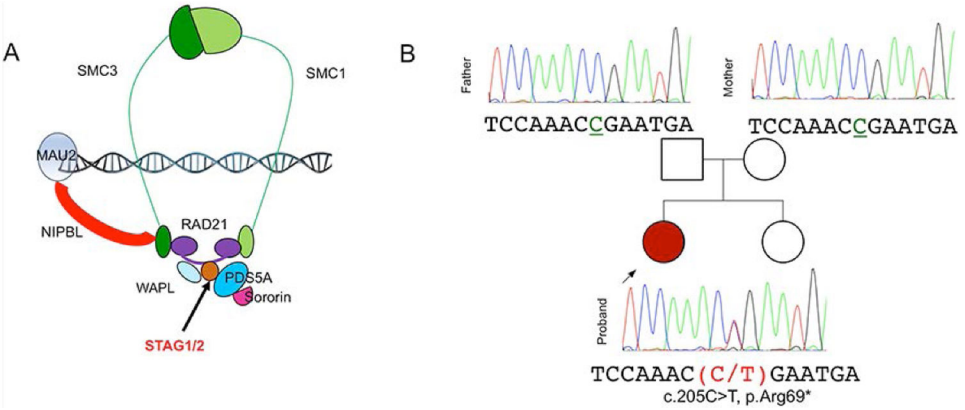

Fig. 1. Characterization of *STAG2* variants

(A) Structure of the cohesin ring and its regulatory proteins. **(B)** Case 1 family pedigree with sequence analysis by Sanger sequencing showed a heterozygous variant, c.205C>T; p.(Arg69*) in Exon 5 of *STAG2* in the affected proband (red).

Author Manuscript Author Manuscript Author Manuscript Author Manuscript

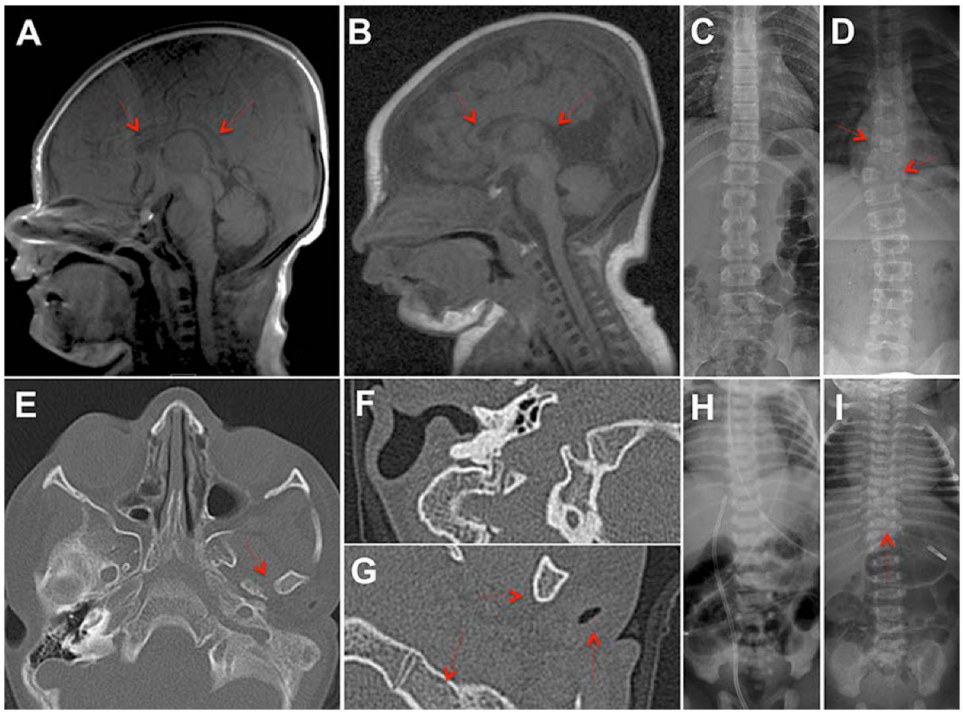

Fig 2. MRI and radiological findings in patients with STAG2 mutations.

(A) Healthy three day old female axial T1 weighted MRI view of a normally developed corpus callosum (red arrows) **(B)** Axial T1 weighted MRI view of patient with STAG2 mutation displaying dysgenesis of the splenium of the corpus callosum (red arrows). **(C)** Chest x-ray of a healthy one day old female demonstrating normal vertebral development. **(D)** Chest x-ray of a patient with STAG2 mutation demonstrating scoliosis and vertebral abnormalities including hemi-vertebrae and “butterfly” vertebrae (red arrows). **(E)** Axial view of bilateral auditory canals in a patient with a STAG2 mutation, showing absence of the left auditory canal (red arrow). **(F)** Higher magnification of the right auditory canal image shows patent canal and normal bone structures **(G)** Higher magnification of the left auditory canal demonstrating external auditory canal atresia with a fused ossicular mass, absent stapes, and severely stenotic oval window (red arrows). **(H)** Chest x-ray of a healthy eight year old female demonstrating normal vertebral development. **(I)** Chest x-ray of a patient with STAG2 mutation demonstrating scoliosis and vertebral abnormalities including hemi-vertebrae (red arrow).

Author Manuscript Author Manuscript Author Manuscript Author Manuscript

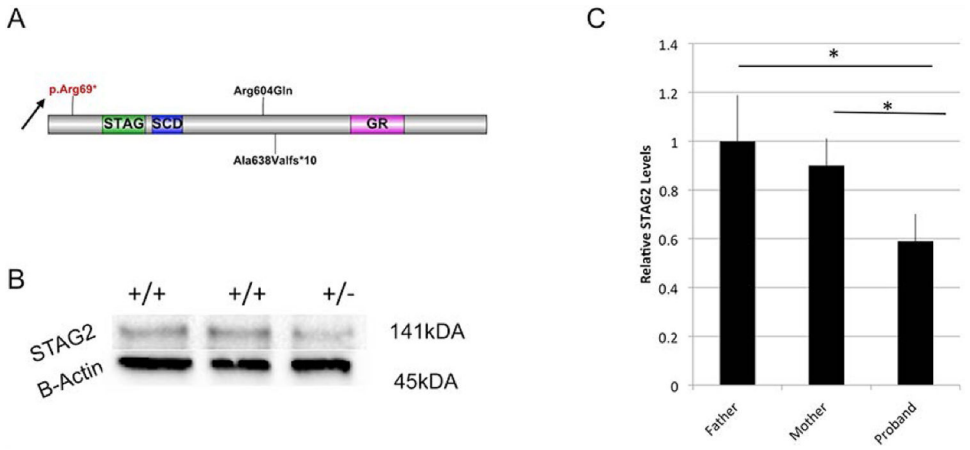

Fig. 3. Location and consequence of STAG2 Variants

(A) Predicted protein domain structure of STAG2. The 1231 amino acid full-length protein is predicted to contain a STAG domain, a stromalin conservative domain (SCD) and a glutamine-rich region domain (GR). The p.Arg69* mutation is indicated by an arrow. The location of the mutations reported by DECIPHER are depicted (p.Arg604Gln and p.Ala638fs*). **(B)** Protein expression analysis of STAG2 in patient and her parents reveals decreased levels in proband (+/−) compared to parents (+/+). **(C)** Western blot analysis was run using two independent antibodies for STAG2. Quantification of band density with normalization to loading controls demonstrates significant reduction in STAG2 levels in the proband when compared to either unaffected parental control. *Denotes significant difference ($p<.05$, Mann-Whitey U Test ($n=6$)).

Author Manuscript Author Manuscript Author Manuscript Author Manuscript

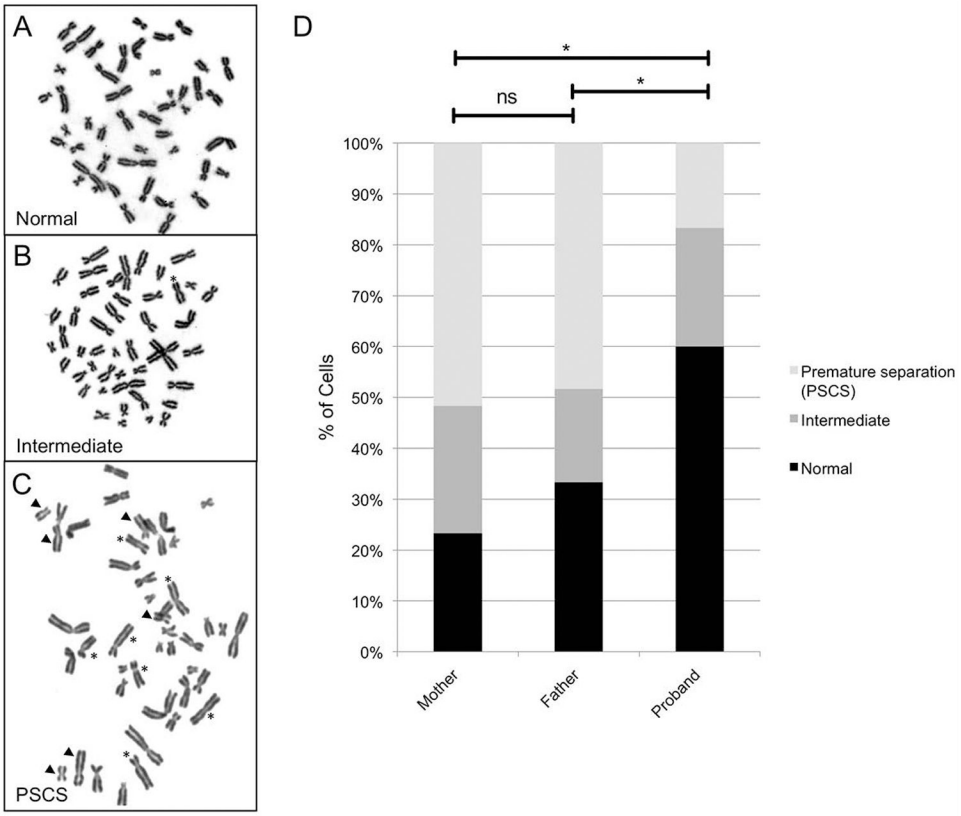

Fig. 4. Sister Chromatid Cohesion Studies on Affected Proband

(A-C) Metaphases that were described as closed, intermediate or having premature sister chromatid separation (PSCS) in our assays. Individual chromatid pairs with abnormal phenotypes are highlighted in **(B)** and **(C)**, with an arrowhead indicating "open" chromatid pairs, an asterisk indicating pairs with "partial" separation, and all other chromatid pairs being "closed." In **(B)** there is one partially separated chromatid pair, while in **(C)** there are 6 open pairs and 7 partial pairs. By our classification, metaphases with 1–2 open/partial chromatid pairs were described as intermediate, and those with 3 or more open/partial chromatid pairs were described as having PSCS. **(D)** A graph showing quantification of these results. 60 metaphases were analyzed from the proband and each parent and classified as described above. In the proband having the *STAG2* mutation, PSCS was not increased; in contrast, the proportion of nuclei having PSCS showed a significant decrease compared to either parent (significance calculated using a two-tailed Fisher's Exact test for mother versus proband (P=0.000029), father versus proband (P=0.00075), and mother versus father (P=0.44779)).

Author Manuscript

Author Manuscript

Author Manuscript

Author Manuscript

Table I

Phenotype abnormality comparison between three cases with *STAG2* variants

		Case 1	Case 2	Case 3
		p.Arg69*	p.Arg604Gln	p.Ala638Valfs*10
Phenotype Abnormalities	**HPO Term**			
Nervous system	HP:0000707	+	+	+
Ear	HP:0000598	+	+	+
Head or neck	HP:0000152	+	+	+
Growth Abnormalities	HP:0001507	+	+	*N*
Limbs	HP:0040064	+	+	*N*
Skeletal system	HP:0000924	+	+	*N*
Abdomen	HP:0001438	*N*	*N*	+
Respiratory system	HP:0002086	*N*	*N*	+

+ = present

- = not present

N =not known

Author Manuscript Author Manuscript Author Manuscript Author Manuscript

Table II

Comparison of *STAG2* variants to phenotypes of other cohesinopathies

	***STAG2* variants**	**CdLS**	**RBS**	**WBS**	**NBS**	**FA**	**CAID**	**CdLS 4**
Gene	***STAG2***	***NIPBL SMC1A HDAC8 SMC3***	***ESCO2***	**DDX11**	***NBN***	***FANCA* & others**	***SGOL1***	***RAD21***
Phenotypes								
Cognitive delay	+	+	+	+	+	+	-	+ (mild)
Growth retardation	+	+	+	+	+	+	+	+
Neuropsychiatric behaviors	+	+	+	+	+	+	−	+
Microcephaly	+	+	+	+	+	+	−	+
Craniofacial dysmorphia *	+	+	+	+	+	+	−	+
Cleft/arched palate	+	+	+	+	+	−	−	+
Syndactyly	+	+	+	+	+	−	−	
Organ abnormalities **	+	+	+	+	+	+	+	+
Cardiac defects	+	+	+	+	−	+	+	−
Limb reductions +	−	+	+	-	+	+	−	−
Hearing loss	+	+	−	+	−	+	−	−
Skin pigmentation abnormalities	−	+	−	+	+	+	+	−
Elevated Cancer incidence	−	−	−	−	+	+	−	−
Bone marrow/hematopoietic defects	−	−	−	−	−	+	−	−

CdLS= Cornelia de Lange syndrome, RBS= Roberts syndrome, WBS=Warsaw breakage syndrome, NBS= Nijmegen Breakage Syndrome, FA=Fanconi Anemia, CAID= Chronic Atrial and Intestinal Dysrhythmia CdLS4=Cornelia de Lange syndrome 4

* Craniofacial dysmorphia include micrognathia, ear abnormalities, wide-set eyes, beaked or prominent nose, arched eyebrows, or low-set ears.

+ Limb reductions are often symmetric. All four limbs are involved in RBS. Limb reduction is predominant in upper extremities in CdLS. Limb reduction appears limited to the radius in NBS and FA.

** Organ abnormalities may include renal, urinary, gonadal, gastroesophageal, and others.